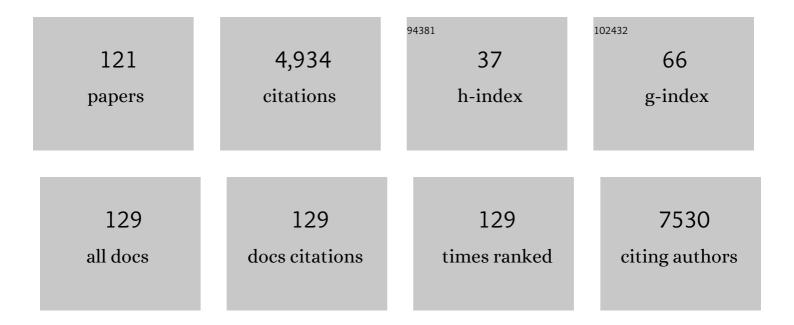
Aldrik H Velders

List of Publications by Year in descending order

Source: https://exaly.com/author-pdf/5710254/publications.pdf Version: 2024-02-01



#	Article	IF	CITATIONS
1	Hollow protein microparticles formed through cross-linking by an Au ³⁺ initiated redox reaction. Journal of Materials Chemistry B, 2022, 10, 6287-6295.	2.9	3
2	Fractionation platform for target identification using off-line directed two-dimensional chromatography, mass spectrometry and nuclear magnetic resonance. Analytica Chimica Acta, 2021, 1142, 28-37.	2.6	5
3	Dendroids, Discrete Covalently Cross-Linked Dendrimer Superstructures. ACS Nano, 2021, 15, 1666-1674.	7.3	14
4	Experiments@home. Nature Reviews Chemistry, 2021, 5, 365-366.	13.8	3
5	Synthesis of D-ï€-A high-emissive 6-arylalkynyl-1,8-naphthalimides for application in Organic Field-Effect Transistors and optical waveguides. Dyes and Pigments, 2021, 191, 109358.	2.0	12
6	Multicompartment dendrimicelles with binary, ternary and quaternary core composition. Nanoscale, 2021, 13, 15422-15430.	2.8	5
7	Syntheses of gold and silver dichroic nanoparticles; looking at the Lycurgus cup colors. Chemistry Teacher International, 2021, 3, .	0.9	11
8	Au ³⁺ -Induced gel network formation of proteins. Soft Matter, 2021, 17, 9682-9688.	1.2	3
9	Oxidant-responsive ferrocene-based cyclodextrin complex coacervate core micelles. Supramolecular Chemistry, 2020, 32, 30-38.	1.5	7
10	Gold and silver dichroic nanocomposite in the quest for 3D printing the Lycurgus cup. Beilstein Journal of Nanotechnology, 2020, 11, 16-23.	1.5	16
11	Dendrimicelles with pH-controlled aggregation number of core-dendrimers and stability. Soft Matter, 2020, 16, 7893-7897.	1.2	8
12	Assessing spatial resolution, acquisition time and signal-to-noise ratio for commercial microimaging systems at 14.1, 17.6 and 22.3AT. Journal of Magnetic Resonance, 2020, 316, 106770.	1.2	5
13	Response of metal-coordination-based polyelectrolyte complex micelles to added ligands and metals. Soft Matter, 2020, 16, 2953-2960.	1.2	7
14	COvalent monolayer patterns in Microfluidics by PLasma etching Open Technology – COMPLOT. Analyst, The, 2020, 145, 1629-1635.	1.7	3
15	Assembly, Disassembly and Reassembly of Complex Coacervate Core Micelles with Redoxâ€Responsive Supramolecular Crossâ€Linkers. ChemSystemsChem, 2020, 2, e1900032.	1.1	4
16	Magnetic Resonance Microscopy at Cellular Resolution and Localised Spectroscopy of Medicago truncatula at 22.3 Tesla. Scientific Reports, 2020, 10, 971.	1.6	13
17	On-Flow Immobilization of Polystyrene Microspheres on β-Cyclodextrin-Patterned Silica Surfaces through Supramolecular Host–Guest Interactions. ACS Applied Materials & Interfaces, 2019, 11, 36221-36231.	4.0	2
18	3D biofilm visualization and quantification on granular bioanodes with magnetic resonance imaging. Water Research, 2019, 167, 115059.	5.3	17

#	Article	IF	CITATIONS
19	Fluorescent imaging of bacterial infections and recent advances made with multimodal radiopharmaceuticals. Clinical and Translational Imaging, 2019, 7, 125-138.	1.1	22
20	Covalently bound monolayer patterns obtained by plasma etching on glass surfaces. Chemical Communications, 2019, 55, 7667-7670.	2.2	5
21	An update on radiotracer development for molecular imaging of bacterial infections. Clinical and Translational Imaging, 2019, 7, 105-124.	1.1	44
22	Regulation of Plasmodium sporozoite motility by formulation components. Malaria Journal, 2019, 18, 155.	0.8	10
23	Self-assembly of oppositely charged polyelectrolyte block copolymers containing short thermoresponsive blocks. Polymer Chemistry, 2019, 10, 3127-3134.	1.9	19
24	Gold nanoparticles embedded in a polymer as a 3D-printable dichroic nanocomposite material. Beilstein Journal of Nanotechnology, 2019, 10, 442-447.	1.5	21
25	Pushing nuclear magnetic resonance sensitivity limits with microfluidics and photo-chemicallyÂinduced dynamic nuclear polarization. Nature Communications, 2018, 9, 108.	5.8	69
26	Illumination of Nanoliter-NMR Spectroscopy Chips for Real-Time Photochemical Reaction Monitoring. Analytical Chemistry, 2018, 90, 1542-1546.	3.2	16
27	Loop-mediated isothermal amplification (LAMP) shield for Arduino DNA detection. BMC Research Notes, 2018, 11, 93.	0.6	29
28	Size-controlled and water-soluble gold nanoparticles using UV-induced ligand exchange and phase transfer. Chemical Communications, 2018, 54, 13355-13358.	2.2	24
29	Cyclodextrin-based complex coacervate core micelles with tuneable supramolecular host–guest, metal-to-ligand and charge interactions. Soft Matter, 2018, 14, 9542-9549.	1.2	10
30	Manipulating and monitoring nanoparticles in micellar thin film superstructures. Nature Communications, 2018, 9, 5207.	5.8	9
31	Nanoparticles reveal Extreme Size-Sorting and Morphologies in Complex Coacervate Superstructures. Scientific Reports, 2018, 8, 13820.	1.6	9
32	Sorting of Molecular Building Blocks from Solution to Surface. Journal of the American Chemical Society, 2018, 140, 8162-8171.	6.6	10
33	Obtaining control of cell surface functionalizations via Pre-targeting and Supramolecular host guest interactions. Scientific Reports, 2017, 7, 39908.	1.6	24
34	Size-Sorting and Pattern Formation of Nanoparticle-Loaded Micellar Superstructures in Biconcave Thin Films. ACS Nano, 2017, 11, 11225-11231.	7.3	23
35	Hydrogel Actuators as Responsive Instruments for Cheap Open Technology (HARICOT). Applied Materials Today, 2017, 9, 271-275.	2.3	23
36	Metal-Free [2 + 2]-Photocycloaddition of (<i>Z</i>)-4-Aryliden-5(4 <i>H</i>)-Oxazolones as Straightforward Synthesis of 1,3-Diaminotruxillic Acid Precursors: Synthetic Scope and Mechanistic Studies. ACS Sustainable Chemistry and Engineering, 2017, 5, 8370-8381.	3.2	20

#	Article	IF	CITATIONS
37	Dendrimer-encapsulated nanoparticle-core micelles as a modular strategy for particle-in-a-box-in-a-box nanostructures. Nanoscale, 2017, 9, 18619-18623.	2.8	22
38	Supramolecular Virusâ€Like Nanorods by Coassembly of a Triblock Polypeptide and Reversible Coordination Polymers. Chemistry - A European Journal, 2017, 23, 239-243.	1.7	13
39	Hybrid Imaging Labels: Providing the Link Between Mass Spectrometry-Based Molecular Pathology and Theranostics. Theranostics, 2017, 7, 624-633.	4.6	12
40	Reaction Pathways in Catechol/Primary Amine Mixtures: A Window on Crosslinking Chemistry. PLoS ONE, 2016, 11, e0166490.	1.1	73
41	Ternary supramolecular quantum-dot network flocculation for selective lectin detection. Nano Research, 2016, 9, 1904-1912.	5.8	9
42	Assembling quantum dots via critical Casimir forces. Solar Energy Materials and Solar Cells, 2016, 158, 154-159.	3.0	20
43	Revealing and tuning the core, structure, properties and function of polymer micelles with lanthanide-coordination complexes. Soft Matter, 2016, 12, 99-105.	1.2	23
44	A clear coat from a water soluble precursor: a bioinspired paint concept. Journal of Materials Chemistry A, 2016, 4, 6868-6877.	5.2	14
45	Simple 3D Printed Scaffoldâ€Removal Method for the Fabrication of Intricate Microfluidic Devices. Advanced Science, 2015, 2, 1500125.	5.6	195
46	2-Amino-4,4α-dihydro-4α,7-dimethyl-3H-phenoxazin-3-one as an unexpected product from reduction of 5-methyl-2-nitrophenol. Tetrahedron Letters, 2015, 56, 1060-1062.	0.7	2
47	Accurate DOSY measure for out-of-equilibrium systems using permutated DOSY (p-DOSY). Journal of Magnetic Resonance, 2015, 258, 12-16.	1.2	23
48	MMP-2/9-Specific Activatable Lifetime Imaging Agent. Sensors, 2015, 15, 11076-11091.	2.1	6
49	Dipeptide recognition in water mediated by mixed monolayer protected gold nanoparticles. Chemical Communications, 2015, 51, 14247-14250.	2.2	31
50	Determination of Kinetic Parameters within a Single Nonisothermal On-Flow Experiment by Nanoliter NMR Spectroscopy. Analytical Chemistry, 2015, 87, 10547-10555.	3.2	25
51	Towards 4th generation biomaterials: a covalent hybrid polymer–ormoglass architecture. Nanoscale, 2015, 7, 15349-15361.	2.8	26
52	Lanthanide-Dipicolinic Acid Coordination Driven Micelles with Enhanced Stability and Tunable Function. Langmuir, 2015, 31, 12251-12259.	1.6	26
53	An Open Source Image Processing Method to Quantitatively Assess Tissue Growth after Non-Invasive Magnetic Resonance Imaging in Human Bone Marrow Stromal Cell Seeded 3D Polymeric Scaffolds. PLoS ONE, 2014, 9, e115000.	1.1	6
54	Multinuclear nanoliter one-dimensional and two-dimensional NMR spectroscopy with a single non-resonant microcoil. Nature Communications, 2014, 5, 3025.	5.8	53

#	Article	IF	CITATIONS
55	Bias induced transition from an ohmic to a non-ohmic interface in supramolecular tunneling junctions with Ga ₂ O ₃ /EGaIn top electrodes. Nanoscale, 2014, 6, 11246-11258.	2.8	41
56	Controlling the number of dendrimers in dendrimicelle nanoconjugates from 1 to more than 100. Soft Matter, 2014, 10, 7337-7345.	1.2	26
57	An activatable, polarity dependent, dual-luminescent imaging agent with a long luminescence lifetime. Chemical Communications, 2014, 50, 9733-9736.	2.2	10
58	Self-assembly triggered by self-assembly: Optically active, paramagnetic micelles encapsulated in protein cage nanoparticles. Journal of Inorganic Biochemistry, 2014, 136, 140-146.	1.5	36
59	Controlled mixing of lanthanide(iii) ions in coacervate core micelles. Chemical Communications, 2013, 49, 3736.	2.2	57
60	Nonlinear Amplification of a Supramolecular Complex at a Multivalent Interface. Angewandte Chemie - International Edition, 2013, 52, 714-719.	7.2	18
61	Evaluation of superparamagnetic iron oxide nanoparticles (Endorem®) as a photoacoustic contrast agent for intraâ€operative nodal staging. Contrast Media and Molecular Imaging, 2013, 8, 83-91.	0.4	63
62	Phosphorescence Imaging of Living Cells with Amino Acid-Functionalized Tris(2-phenylpyridine)iridium(III) Complexes. Inorganic Chemistry, 2012, 51, 2105-2114.	1.9	70
63	Electronâ€Induced Dynamics of Heptathioether β yclodextrin Molecules. Small, 2012, 8, 317-322.	5.2	3
64	Tunable doping of a metal with molecular spins. Nature Nanotechnology, 2012, 7, 232-236.	15.6	29
65	Structure–Photoluminescence Quenching Relationships of Iridium(III)–Tris(phenylpyridine) Complexes. European Journal of Inorganic Chemistry, 2012, 2012, 1025-1037.	1.0	8
66	Biomimetic Crystallization of Ag ₂ S Nanoclusters in Nanopore Assemblies. Journal of the American Chemical Society, 2011, 133, 2875-2877.	6.6	38
67	Lateral interactions at functional monolayers. Journal of Materials Chemistry, 2011, 21, 2428-2444.	6.7	24
68	Self-Complementary Recognition of Supramolecular Urea–Aminotriazines in Solution and on Surfaces. Langmuir, 2011, 27, 14272-14278.	1.6	12
69	Small-Volume Nuclear Magnetic Resonance Spectroscopy. Annual Review of Analytical Chemistry, 2011, 4, 227-249.	2.8	88
70	Reactivity of 2-formylphenylboronic acid toward secondary aromatic amines in amination–reduction reactions. Tetrahedron Letters, 2011, 52, 6639-6642.	0.7	19
71	Interaction of dioxygen with the electronic excited state of Ir(III) and Ru(II) complexes: Principles and biomedical applications. Coordination Chemistry Reviews, 2011, 255, 2542-2554.	9.5	117
72	Supramolecular Au Nanoparticle Assemblies as Optical Probes for Enzyme‣inked Immunoassays. Small, 2011, 7, 66-69.	5.2	39

#	Article	IF	CITATIONS
73	Strategies for Patterning Biomolecules with Dipâ€Pen Nanolithography. Small, 2011, 7, 989-1002.	5.2	101
74	Patterning: Strategies for Patterning Biomolecules with Dip-Pen Nanolithography (Small 8/2011). Small, 2011, 7, 982-982.	5.2	3
75	CCVD Synthesis of Carbonâ€Encapsulated Cobalt Nanoparticles for Biomedical Applications. Advanced Functional Materials, 2011, 21, 3583-3588.	7.8	39
76	Multivalent Nanoparticle Networks as Ultrasensitive Enzyme Sensors. Angewandte Chemie - International Edition, 2011, 50, 5704-5707.	7.2	68
77	Dendritic Ruthenium(II)â€Based Dyes Tuneable for Diagnostic or Therapeutic Applications. Chemistry - A European Journal, 2011, 17, 464-467.	1.7	32
78	Peptideâ€Functionalized Luminescent Iridium Complexes for Lifetime Imaging of CXCR4 Expression. ChemBioChem, 2011, 12, 1897-1903.	1.3	43
79	Ratiometric Fluorescent Detection of an Anthrax Biomarker at Molecular Printboards. Angewandte Chemie - International Edition, 2010, 49, 5938-5941.	7.2	100
80	Control over Rectification in Supramolecular Tunneling Junctions. Angewandte Chemie - International Edition, 2010, 49, 10176-10180.	7.2	26
81	Diverse reactivity of 2-formylphenylboronic acid with secondary amines: synthesis of 3-amino-substituted benzoxaboroles. Tetrahedron Letters, 2010, 51, 6181-6185.	0.7	30
82	Mathematically defined tissue engineering scaffold architectures prepared by stereolithography. Biomaterials, 2010, 31, 6909-6916.	5.7	437
83	Visualizing Resonance Energy Transfer in Supramolecular Surface Patterns of <i>l²</i> â€CDâ€Functionalized Quantum Dot Hosts and Organic Dye Guests by Fluorescence Lifetime Imaging. Small, 2010, 6, 2870-2876.	5.2	12
84	Energy transfer: Visualizing Resonance Energy Transfer in Supramolecular Surface Patterns of β-CD-Functionalized Quantum Dot Hosts and Organic Dye Guests by Fluorescence Lifetime Imaging (Small 24/2010). Small, 2010, 6, 2869-2869.	5.2	0
85	A Coordination Cage with an Adaptable Cavity Size. Journal of the American Chemical Society, 2010, 132, 14004-14005.	6.6	184
86	Ferrocene-coated CdSe/ZnS quantum dots as electroactive nanoparticles hybrids. Nanotechnology, 2010, 21, 285703.	1.3	17
87	Pyrylium monolayers as amino-reactive platform. Chemical Communications, 2010, 46, 4193.	2.2	22
88	Fabrication and Luminescence of Designer Surface Patterns with β-Cyclodextrin Functionalized Quantum Dots via Multivalent Supramolecular Coupling. ACS Nano, 2010, 4, 137-142.	7.3	68
89	Multimodal Tumor-Targeting Peptides Functionalized with Both a Radio- and a Fluorescent Label. Bioconjugate Chemistry, 2010, 21, 1709-1719.	1.8	104
90	Protein Immobilization on Ni(II) Ion Patterns Prepared by Microcontact Printing and Dip-Pen Nanolithography. ACS Nano, 2010, 4, 1083-1091.	7.3	31

#	Article	IF	CITATIONS
91	An iridium(iii)-caged complex with low oxygen quenching. Chemical Communications, 2010, 46, 6726.	2.2	23
92	Orthogonal Covalent and Noncovalent Functionalization of Cyclodextrin-Alkyne Patterned Surfaces. Journal of the American Chemical Society, 2010, 132, 11434-11436.	6.6	58
93	Photo-Cross-Linked Poly(<scp>dl</scp> -lactide)-Based Networks. Structural Characterization by HR-MAS NMR Spectroscopy and Hydrolytic Degradation Behavior. Macromolecules, 2010, 43, 8570-8579.	2.2	32
94	On-line monitoring of a microwave-assisted chemical reaction by nanolitre NMR-spectroscopy. Chemical Communications, 2010, 46, 4514.	2.2	46
95	Magnetic Detection of the Sentinel Lymph Node in Ex Vivo Tissue with Colorectal Cancer. IFMBE Proceedings, 2010, , 447-449.	0.2	2
96	The Formation of Largeâ€Area Conducting Grapheneâ€Like Platelets. Chemistry - A European Journal, 2009, 15, 8235-8240.	1.7	76
97	Chiral Salan Aluminium Ethyl Complexes and Their Application in Lactide Polymerization. Chemistry - A European Journal, 2009, 15, 9836-9845.	1.7	164
98	Expression of Sensitized Eu ³⁺ Luminescence at a Multivalent Interface. Journal of the American Chemical Society, 2009, 131, 12567-12569.	6.6	44
99	Reversible Phase Transfer of (CdSe/ZnS) Quantum Dots between Organic and Aqueous Solutions. ACS Nano, 2009, 3, 661-667.	7.3	124
100	NMR Characterization of Fourth-Generation PAMAM Dendrimers in the Presence and Absence of Palladium Dendrimer-Encapsulated Nanoparticles. Journal of the American Chemical Society, 2009, 131, 341-350.	6.6	104
101	Polymerization of Lactide Using Achiral Bis(pyrrolidene) Schiff Base Aluminum Complexes. Macromolecules, 2009, 42, 1058-1066.	2.2	131
102	Photoluminescence Quenching of CdSe/ZnS Quantum Dots by Molecular Ferrocene and Ferrocenyl Thiol Ligands. Journal of Physical Chemistry C, 2009, 113, 18676-18680.	1.5	43
103	Porous Multilayer-Coated AFM Tips for Dip-Pen Nanolithography of Proteins. Journal of the American Chemical Society, 2009, 131, 7526-7527.	6.6	36
104	Flavonol 3- <i>O</i> -Glycosides Series of <i>Vitis vinifera</i> Cv. Petit Verdot Red Wine Grapes. Journal of Agricultural and Food Chemistry, 2009, 57, 209-219.	2.4	178
105	Nanoparticle Size Determination by ¹ H NMR Spectroscopy. Journal of the American Chemical Society, 2009, 131, 14634-14635.	6.6	46
106	Supramolecular Interactions at the Picomole Level Studied by ¹⁹ F NMR Spectroscopy in a Microfluidic Chip. Small, 2008, 4, 1293-1295.	5.2	13
107	Fabrication and Visualization of Metalâ€ion Patterns on Glass by Dipâ€Pen Nanolithography. ChemPhysChem, 2008, 9, 1680-1687.	1.0	16
108	Imidazolide monolayers for reactive microcontact printing. Journal of Materials Chemistry, 2008, 18, 4959.	6.7	9

#	Article	IF	CITATIONS
109	N-MethylbenzimidazoleN-methylbenzimidazolium hexafluorophosphate. Acta Crystallographica Section E: Structure Reports Online, 2006, 62, o21-o23.	0.2	2
110	Ligands Rock & Roll: Stepwise Twisting of Twocis-Coordinated Lopsided N-Heterocycles in an Octahedral Bis(2-phenylazopyridine)-Ruthenium(II) Complex with Seven Atropisomers. Chemistry - A European Journal, 2005, 11, 1325-1340.	1.7	6
111	Thiacalix[4]arene derivatives as radium ionophores: a study on the requirements for Ra2+ extraction. Organic and Biomolecular Chemistry, 2005, 3, 1993.	1.5	13
112	Dichlorobis(2-phenylazopyridine)ruthenium(ii) complexes: characterisation, spectroscopic and structural properties of four isomers. Dalton Transactions, 2004, , 448-455.	1.6	45
113	Synthesis and Chemicalâ [°] Pharmacological Characterization of the Antimetastatic NAMI-A-Type Ru(III) Complexes (Hdmtp)[trans-RuCl4(dmso-S)(dmtp)], (Na)[trans-RuCl4(dmso-S)(dmtp)], and [mer-RuCl3(H2O)(dmso-S)(dmtp)] (dmtp = 5,7-Dimethyl[1,2,4]triazolo[1,5-a]pyrimidine). Journal of Medicinal Chemistry, 2004, 47, 1110-1121.	2.9	118
114	New Cytotoxic and Water-Soluble Bis(2-phenylazopyridine)ruthenium(II) Complexes. Journal of Medicinal Chemistry, 2003, 46, 1743-1750.	2.9	78
115	Crystallographic and NMR evidence of the unusual N6,N7-didentate chelation of 3-methyladenine coordinated to the cytotoxic î±-dichlorobis(2-phenylazopyridine)ruthenium(ii) complex. Dalton Transactions RSC, 2002, , 2809.	2.3	10
116	Structure-independent cross-validation between residual dipolar couplings originating from internal and external orienting media. Journal of Biomolecular NMR, 2002, 22, 365-368.	1.6	14
117	Strong Differences in the in Vitro Cytotoxicity of Three Isomeric Dichlorobis(2-phenylazopyridine)ruthenium(II) Complexes. Inorganic Chemistry, 2000, 39, 2966-2967.	1.9	184
118	Tuning the Rotational Behavior of Lopsided Heterocyclic Nitrogen Ligands (L) in Octahedral cis-[Ru(bpy)2(L)2](PF6)2 Complexes. A Variable-Temperature 1H NMR Study. Inorganic Chemistry, 2000, 39, 4073-4080.	1.9	27
119	Synthesis, Characterization, and Crystal Structure of α-[Ru(azpy)2(NO3)2] (azpy = 2-(Phenylazo)pyridine) and the Products of Its Reactions with Guanine Derivatives. Inorganic Chemistry, 2000, 39, 3838-3844.	1.9	79
120	A Unique Fourfold Intramolecular Hydrogen Bonding Stabilises the Structure oftrans-Bis(2-amino-5,7-dimethyl[1,2,4]triazolo[1,5-a]pyrimidine-N3)aquatrichlororuthenium(III) Monohydrate. European Journal of Inorganic Chemistry, 1999, 1999, 213-215.	1.0	25
121	The First Observation and Full Characterization of All Atropisomers and Their Allowed Interconversions in an Octahedral Bis(bipyridine)ruthenium(II) Complex with Two Lopsided Bicyclic Ligands, as Studied by 2D NMR Techniques at Variable Temperature. Inorganic Chemistry, 1999, 38, 2762-2763.	1.9	26